Available online at www.sciencedirect.com
SCIENCE DIRECT®
Polymer 45 (2004) 1647–1657
polymer
www.elsevier.com/locate/polymer

The effect of fluorinated side chain attached on hard segment on the phase separation and surface topography of polyurethanes

Hong Tan, Min Guo, Rongni Du, Xingyi Xie, Jiehua Li, Yinping Zhong, Qiang Fu*

Department of Polymer Science and Materials, College of Polymer Science and Engineering, State key Laboratory of Polymer Materials Engineering, Sichuan University, Chengdu 610065, People's Republic of China

Received 18 August 2003; accepted 22 December 2003

Abstract

It has been well established that polyurethanes exhibit a two-phase micro-structure due to the thermodynamic incompatibility between the soft segments and hard segments. In this work, we reported the effect of fluorinated side chain attached on hard segment on the phase separation and surface topography of polyurethanes. Two sets of fluorinated polyurethanes, namely, poly(ether urethane)s and poly(carbonate urethane)s containing various amounts of chain extender of fluorinated side chains, were investigated by DSC, XPS, DMA, AFM and FTIR. It was found that the phase separation in both bulk and surface increases in fluorinated poly(carbonate urethane)s and the phase mixing increases in fluorinated poly(ether urethane)s, with increasing amounts of fluorinated side chain. The increased degree of hydrogen bonding between hard segments and soft segments was observed by FTIR for fluorinated poly(ether urethane), which is believed to result in the enhanced phase mixing, and the enhanced association of domains with long-range order (hydrogen bonding) between hard segments was evident for fluorinated poly(carbonate urethane)s, which may correspond to the enhanced phase separation. The result is new and provides direct connection between surface topography and bulk phase separation of polyurethanes.

Keywords: Phase separation; Hydrogen bonding; Fluorinated polyurethane

1. Introduction

Polyurethanes (PUs) are widely used as biomedical materials because of their excellent mechanical properties and good blood compatibility [1]. These desirable bulk properties mainly derive from the two-phase structure of hard and soft domains: hard domains, composed of aromatic (or aliphatic) urethane or urea segments, and soft domains, composed of aliphatic polyether, polycarbonate, polyester or poly(methylsiloxane) segments [2,3]. Factors that control the phase separation include composition, such as the symmetry of diisocyanate, the type of chain extender, the number of carbons in linear low molecular weight chain extender [4], the type and the chain lengths of soft segments [2,4–6], crystallizability of either segment [7], the thermal history of the polyurethanes [5,8,9] and the method of synthesis [10].

Recently, extensive work has been done on the fluorinated polyurethanes, due to their unique low surface energies [11,12], biocompatibility and biostability [13–16], low water absorptivity, lubricity, thermal and oxidative stability and nonsticking behavior [17]. However, the incorporation of fluorine in polyurethanes has been shown to result in the migration of the fluorine group to the surface driven by the low surface energy of the fluorinated chain, which makes the surface morphology of polyurethane much complicated. The surface structures of fluorinated polyurethanes were studied extensively [11,12,18–27]. The surface phase separated morphology of the poly(carbonate urethane)s containing fluorinated polyether was observed by Kim Y. S. et al. [21], and the similar surface phase morphology about 10 nm near the surface was also observed in normal polyurethanes [28,29]. However, Honeychuck R.V. et al. did not observe the surface phase separation in fluorinated polyurethanes based on a series of ethylene–fluoroakyl-ethylene diols and HDI [27]. On the other hand, the bulk structure of the fluorinated polyurethanes has also intensively investigated [22–26,30–32]. Tonelli et al. [30–32] in their study of the fluorinated polyurethanes composed of MDI, 1,4-butanediol (BDO) and perfluoropolyether

* Corresponding author. Tel.: +86-288-546-0953; fax: +86-28-85405402.
E-mail address: qiangfu@scu.edu.cn (Q. Fu).

0032-3861/$ - see front matter © 2004 Elsevier Ltd. All rights reserved.
doi:10.1016/j.polymer.2003.12.064

(PFPE), observed that the phase separation occurred due to the incompatibility of the fluorinated soft and the hard segments, and that synthesis methods affected the morphology and microstructure. For multiblock fluorinated polyurethanes which have a wide distribution of block lengths, Yoon and Ratner [22] studied the bulk structure of poly(ether urethanes) and poly(ether urethane ureas) with various perfluorinated chain extenders and also noticed that the surface topography of such polymers depended strongly on the extent of the phase separation. They concluded that the existence of discrete domains on the surface of these fluorinated polyurethanes was improbable. Thomas et al. [33,34] studied the diblock and triblock components of different polarity and configuration in a covalently linked block system, and revealed an enriching phenomenon of certain components at the surface. The enrichment at the surface can be governed by the bulk structure, the degree of phase separation near the surface, and the surface free energy difference between the two components.

In our previous studies [35], a series of fluorinated polyurethanes were synthesized with fluorinated side chain attached on hard segment. The fluorine group was found to easily migrate to the surfaces of polyurethanes when the amount of fluorinated side chain was small. So it is significant to further investigate the bulk structure and the extent of micro-phase separation at the surface of these multiblock fluorinated polyurethanes in order to understand the effect of fluorinated side chain attached on hard segment on the bulk structure and surface topography. In this paper, we report the effect of fluorinated side chain attached on hard segment on the bulk structure and the surface structure of the fluorinated polyurethanes, the relationship between bulk structure and surface structure was characterized by DSC, DMA, FTIR, XPS and AFM.

2. Experimental

2.1. Synthesis of materials

A series of poly(ether urethane)s and poly(carbonate urethane)s containing various amounts of chain extender with fluorinated side chains were synthesized with methylenebis(phenylene isocyanate) (MDI), polytetramethyleneoxide (PTMO), or poly(1,6-hexyl-1,5-pentylcarbonate) diol (PHPCD), 1,4-butandiol (BDO) and 3-(2,2,3,3,4,4,5,5,6,6,7,7,8,8,8-pentadecafluoro-octyloxy)-propane-1,2-diol (PFOPDOL). The details of the fluorinated polyurethanes synthesis were reported in Ref [35] and the detailed information of these samples is listed in Table 1, and the structure is shown in Fig. 1.

2.2. DSC measurements

The polymer samples (17–20 mg) were cut off from the films prepared by casting the polymer onto a clean glass disk from 10% (w/v) THF or mixture solvent of THF and DMAc (5:1), putting into oven at 40 °C for 24 h, 50 °C for 12 h and 60 °C for 3 days under vacuum. Because THF can not completely dissolve the poly(carbonate urethane)s, DMAc was added to help the dissolution. There should be no remarkable effect of THF and DMAc on fluorinated polyurethanes surfaces as long as the solvent is removal completely (the same as for other characteration). Moreover, there are not markedly effects of THF and DMAc on fluorinated polyurethanes surfaces [24]. The DSC heating data was collected at 10 °C/min from −100 to 80 °C by TA instrument 2910 thermal analyzer, and from 50 to 220 °C by a Perkin–Elmer differential scanning calorimeter (Pyris 1 DSC).

2.3. Dynamic mechanical analysis (DMA)

Dynamic mechanical properties were measured on a Dynamic Mechanical Thermal Analyzer (DMTA IV Rheometric Scientific LTD) using rectangular test film specimens ($45 \times 10 \times 0.2\ mm^3$) prepared as described above. The testing was done at a heating rate of 5 °C/min and at a frequency of 10 Hz.

2.4. Fourier transform infrared spectroscopy (FTIR)

Each sample for infrared analysis was prepared by casting the polymer onto a clean potassium bromide disc

Table 1
Composition of segmented poly(ether urethane)s and poly(carbonate urethane)s with various amounts of fluorinated chain extender

Sample	Molar ratio MDI/chain extender/PTMO (or PHPCD)	Chain extender BDO, PFOPDOL (mol)	Hard segment (wt%)	Fluorine (at.%)[a]
PEU	2:1:1	1.0, 0.0	37.1	0.0
FPEU20	2:1:1	0.8, 0.2	40.0	2.6
FPEU50	2:1:1	0.5, 0.5	43.9	6.0
FPEU100	2:1:1	0.0, 1.0	49.3	11.1
PHPCPU	2:1:1	1.0, 0.0	35.8	0.00
FPHPCPU20	2:1:1	0.8, 0.2	38.7	2.4
FPHPCPU50	2:1:1	0.5, 0.5	42.5	5.7
FPHPCPU100	2:1:1	0.0, 1.0	47.9	10.5

[a] Atomic percentage of fluorine.

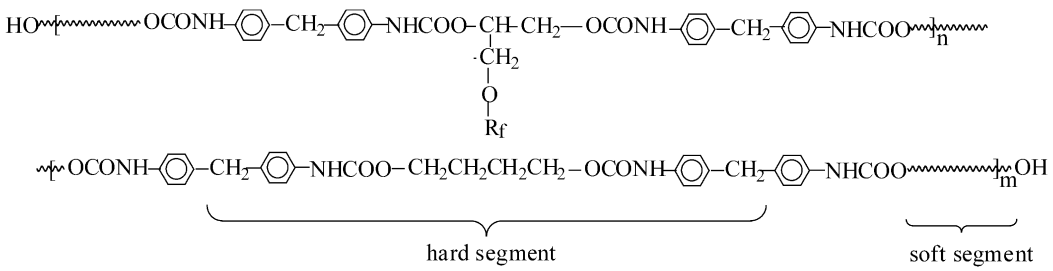

Fig. 1. Structure of fluoropolyurethanes. Rf = $CH_2(CF_2)_6CF_3$; $n = 1, 2, 3,\ldots$, $m = 0, 1, 2, 3,\ldots$. Soft segment is PTMO or PHPCD.

from a single drop of 1% (w/v) THF or a mixture of the solvents THF and DMAc (5:1). These samples were put into an oven at 40 °C for 24 h, 50 °C for 12 h, and 60 °C for 24 h under vacuum to completely remove the solvent. Infrared data was obtained with the Nicolet-560 spectrophotometer between 4000 and 600 cm^{-1} in the resolution of 4 cm^{-1}. Fifty scans were averaged for each sample. The analysis was performed to fit the combination of Lorentzian and Guassian curve by peaksolve™ version1.05 (Galactic Industries Corporation).

2.5. Atomic force microscopy

AFM sample films were prepared by casting the poly(ether urethane)s onto clean glass disks from 10% (w/v) THF and the poly(carbonate urethane)s from 5% (w/v) DMAc. The disks were put into an oven at 40 °C for 24 h, 50 °C for 12 h, and 60 °C for 3 days under vacuum. The AFM measurements were performed on SPA400 with an SPI3800N controller, Seiko Instruments Industry, Co., Ltd. at room temperature, using the micro-fabrication cantilevers with force constant of approximately 13 N/m. In tapping mode, the topographic and phase data were recorded simultaneously. For our study, the ratio of amplitude was adjusted to 0.8–0.9 of the free air amplitude for all the images. Under this light force tapping conditions, phase data is sensitive to local hydrophilicity differences of the phase about 0–5 nm below the surface. Hydrophobic region are bright in phase images and dark in topography images [36–38].

2.6. X-ray photoelectron spectroscopy (XPS)

XPS was carried out on an XSAM-800 electron spectrometer. The spectrometer was equipped with a Mg Kα achromatic X-ray source (20 kV, 10 mA) and take-off angles of 30° was used with X-ray source. Each sample for XPS was prepared by casting the polymer onto a clean silicon wafer from 10% (w/v) THF or a mixture of the solvents THF and DMAc (5:1). The disks were put into an oven at 40 °C for 24 h, 50 °C for 12 h, and 60 °C for 3 days under vacuum.

3. Results and discussion

3.1. The bulk phase separation of fluorinated polyurethanes

3.1.1. DSC analysis

The glass transition temperatures (T_g) and the melting endotherms of the fluorinated poly(ether urethane)s are showed in Fig. 2. The T_gs and other thermal characteristics results are summarized in Table 2. In the poly(ether urethane) system, one T_g is observed in each sample (Fig. 2A), and increases with an increasing in fluorine content. The change of T_g of the soft segment has been used as an

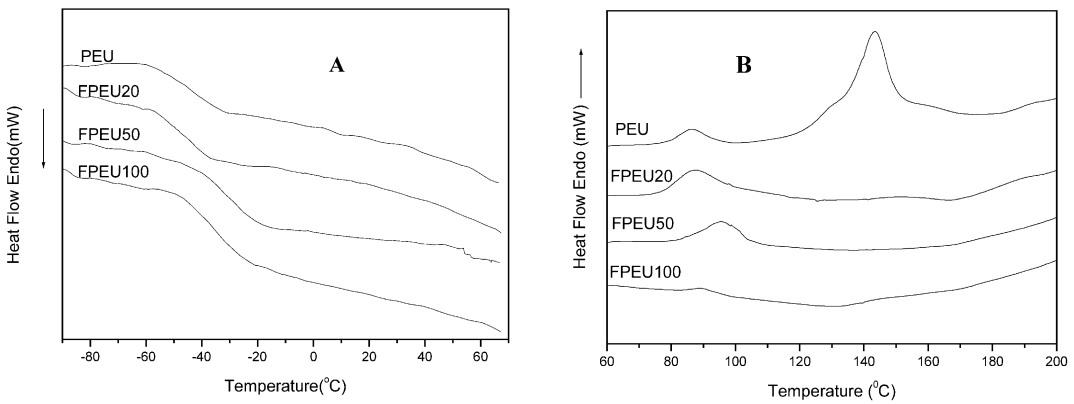

Fig. 2. DSC thermogrames of fluorinated poly(ether urethane)s and poly(ether urethane)s. A: temperature range from − 100 to 70 °C. B: temperature range from 60 to 200 °C.

Table 2
Transition temperatures and enthalpies of the polyurthanes and fluorinated polyurethanes

Sample	T_g (soft) (°C)	T_1 (°C)	$\Delta H1$ (J/g)	T_2 (°C)	$\Delta H2$ (J/g)
PEU	−45.2	85.998	0.771	143.436	4.097
FPEU20	−45.14	87.606	1.895	–	–
FPEU50	−33.41	99.612	1.724	–	–
FPEU100	−37.15	89.514	0.271	–	–
PHPCPU	−3.62	119.668	6.501	–	–
FPHPCPU20	1.51	93.080	0.861	141.879	0.716
FPHPCPU50	−7.52	90.713	0.584	136.518	0.517
FPHPCPU100	−8.95	101.269	0.309	135.938	0.464

indicator of the degree of phase separation [6]. The increasing of T_g of fluorinated poly(ether urethane)s compared with that of the PEU indicates that the phase separation of fluorinated poly(ether urethane)s is getting less as the content of fluorine attached on hard block increases. On the other hand, two DSC melting endotherms are observed at temperature ranging between 74–96 °C and 131–155 °C for poly(ether urethane) (Fig. 2B), high temperature peak is seen to disappear for all the fluorinated poly(ether urethane)s. According to previous literature [8], the endotherm at lower temperature is attributed to the disruption of domains with limited short-range order, and the transition at higher temperature represents the dissociation of domains containing long-range order. Our result suggests that mixing between soft and hard segments is enhanced with increasing content of fluorine attached on hard block in poly(ether urethane)s, and no association of domains with long-range order exists any more.

For the fluorinated poly(carbonate urethane)s, one also observes one T_g in both PHPCPU and FPHPCPUs (Fig. 3A, Table 2). The T_g of FPHPCPUs decreases compared with PHPCPU and. One observes also obviously two melting endothermal peaks in fluorinated poly(carbonate urethane)s (Fig. 3B, Table 2). The low melting peak keeps relatively constant but a great increase in the high melting peaks is seen after introducing fluorine on the hard segments. This result indicates that the association of domains with long-range order becomes much stronger in FPHPCPUs.

3.1.2. Dynamic mechanical analysis

Dynamic mechanical analysis provides information on glass transition, phase separation and the mechanical behavior of a polymer. The dynamic mechanical properties of the fluorinated poly(ether urethane)s series are showed in Fig. 4. From the storage modulus (E') vs. temperature curves (Fig. 4A), the storage modulus in the rubbery plateau region of PEU is higher than that of fluorinated poly(ether urethane)s, and the loss peaks of fluorinated poly(ether urethane)s are shifted toward higher temperature (Fig. 4B). Fig. 5 shows the dynamic mechanical properties of the fluorinated poly(carbonate urethane)s series. The storage modulus in the rubbery plateau region of FPHPCPU50 is the highest in poly(carbonate urethane)s series (Fig. 5A), and the loss peaks of fluorinated poly(carbonate urethane)s are shifted toward lower temperature (Fig. 5B). Numerical DMA data of all polyurethanes are reported in Table 3. In order to better understanding the effect of fluorinated side chain attached on hard segment on the bulk phase separation, the relationship between the amount of chain extender PDFDOL and the rubber plateau modulus (at temperature $T_g + 50$ °C) [31], T_g and dissipation factor (tan δ) were considered, respectively. For poly(ether urethane)s series, the storage modulus (E') decreased, T_g increased and tan δ increased with the amount of chain extender PDFDOL increasing (Fig. 6). However, for poly(carbonate urethane)s series, these changes are appropriately in reverse to those of poly(ether urethane)s (Fig. 6). The increase in storage modulus of fluorinated poly(carbonate urethane) indicates that the hard-segment acts as reinforcing agent more efficiently via enhanced phase separation [31]. On the other hand, the rise in tan δ of fluorinated poly(ether urethane)s indicates that interaction between hard segment and soft segment is enhanced. The results indicate that the degree of phase separation decreases in poly(ether urethane) system but increases in

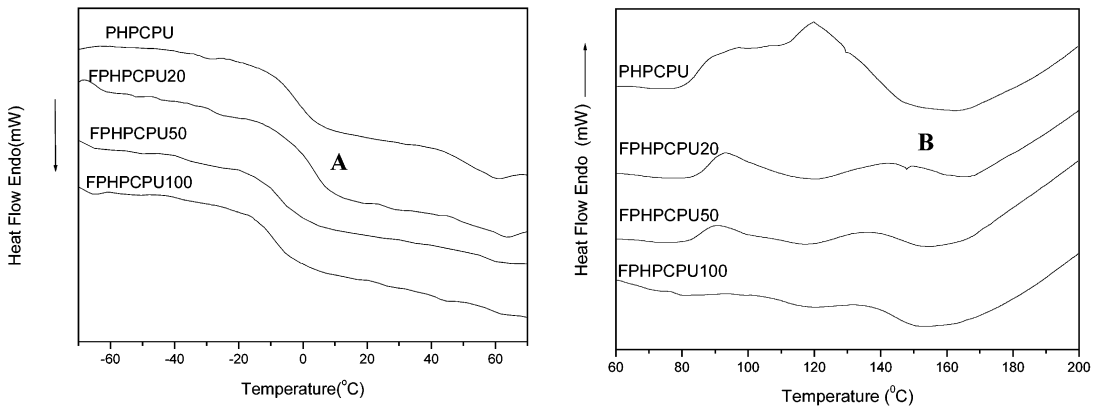

Fig. 3. DSC thermogrames of fluorinated poly(carbonate urethane)s and poly(carbonate urethane)s. A: temperature range from − 100 to 80 °C. B: temperature range from 60 to 200 °C.

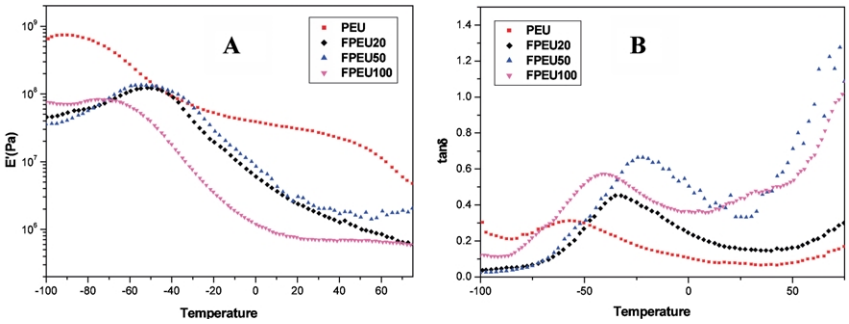

Fig. 4. Dynamic-mechanical spectra for fluorinated poly(ether urethane)s and poly(ether urethane)s samples. A: E' vs. T, B: tan δ vs. T.

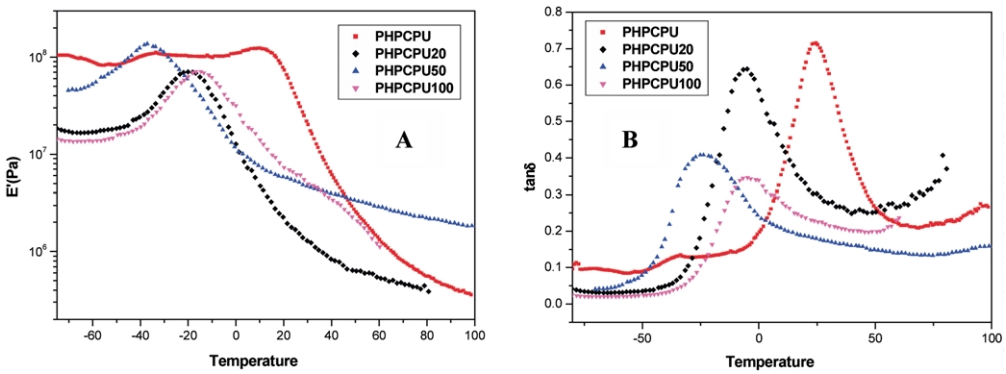

Fig. 5. Dynamic-mechanical spectra for fluorinated poly(carbonate urethane)s and poly((carbonate urethane)s samples. A: E' vs. T, B: tan δ vs. T.

poly(carbonate urethane) system with increasing fluorine content. DMA result is in good agreement with DSC data.

3.2. The surface phase separation of fluorinated polyurethanes

3.2.1. XPS analysis

In the XPS measurement, the sample is irradiated with Mg Kα achromatic X-ray as the kinetic energy of the emitted photoelectron is recorded. The analysis depth, d is controlled by the mean free path [39] of the ejected photoelectron according to the following equation [40]

$$d = 3\lambda \sin \theta$$

where λ is the inelastic mean free path of electron and θ is the take-off angle (between the film surface and the axis of analyzer lens). For typical polymer systems, the take-off angle represents the depth having been detected. 30° is near the surface (5 nm) and 90° is ten nanometers away from the surface, In our experiments, the take-off angle was 30°, and the detection depth is then around 5 nm. The XPS result is listed in Table 4, and all of the fluorinated polyurethanes films have higher fluorine on the surfaces compared with that in the bulk (see Table 1). For the series of fluorinated poly(ether urethane)s, the FPEU20 has the highest atomic percentage of fluorine, F/O and F/C atomic ratio at the depth of about 5 nm. On the other hand, for the series of fluorinated poly(carbonate urethane)s, the FPHPCPU50 has the highest atomic percentage of fluorine, F/O and F/C atomic ratio at the depth of about 5 nm. In the mean time, all of these sample films have high fluorine enrichment factor, especially, for FPEU20 and FPHPCPU20 (Table 4). The XPS result suggests that the surfaces of fluorinated polyurethanes are nonpolar and this has been verified by contact angle measurement with water [35]. It should be noted that the amount of nitrogen and elemental fluorine at surface represents the amount of hard block and fluorinated side chain migrating to the surface, respectively. The amount of surface elemental nitrogen increases with increasing amount of the fluorinated side chain of the chain extender PFOPDOL (Table 4), which indicates that more and more hard segments have been pulled to the surfaces with the help of fluorinated side chains.

Table 3
The storage modulus at $T_g + 50$ °C, dissipation factor and glass transition temperature of fluorinated polyurethanes in DMA

	E' (MPa) ($T_g + 50$ °C)	tan δ	T_g (°C)
PEU	7.63	0.31	−57.35
FPEU20	7.18	0.45	−31.85
FPEU50	6.83	0.66	−21.92
FPEU100	6.39	0.57	−40.12
PHPCPU	6.47	0.73	24.5
FPHPCPU20	6.45	0.64	−5.0
FPHPCPU50	7.46	0.41	−23.7
FPHPCPU100	7.14	0.34	−4.86

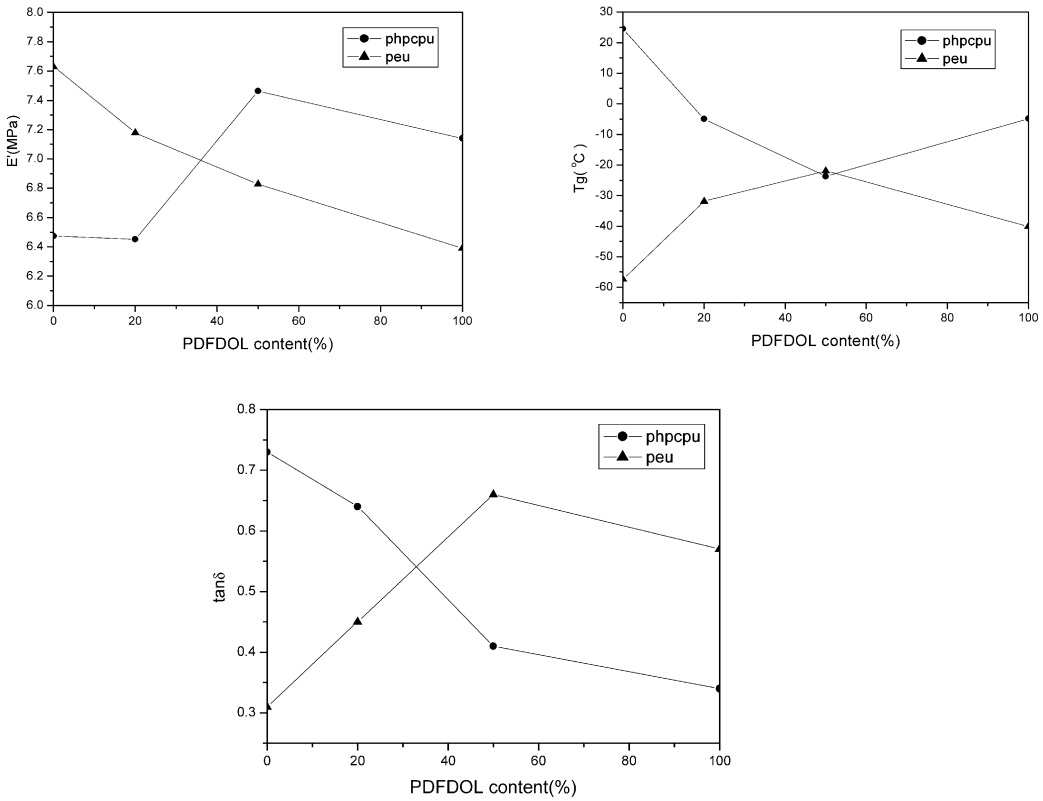

Fig. 6. Relationship between dynamic mechanical properties and molar percentage content of PDFDOL in chain extender of fluorinated polyurethanes, A: the storage modulus (E') at $T_g + 50$ °C vs. content of PDFDOL, B: dissipation factor (tan δ) vs. content of PDFDOL,and C: glass transition temperature (T_g) vs. content of PDFDOL.

3.2.2. AFM measurement

AFM technique was used to study the microdomains of polyurethanes lying underneath the upper most surface layer by moderate force tapping [21,28,29], and the phase imaging at moderate tapping of the ratio (amplitudes with range 0.4–0.7) provides information about surface stiffness variation related to changes in Young's modulus [28,36]. However, the phase imaging at light force tapping of the ratio of amplitudes with range 0.8–0.9 derives the chemical resolution from hydrophilicity differences of the phase at the surface [36–38]. For some fluorinated polymer surfaces, the fluorine level at about 5 nm depth is about ten-fold above their stoichiometric level and the concentration profile of fluorine exhibits a steep gradient normal to the surface [21, 41]. I should be also pointed out that AFM study of surface morphology in phase separated polyurethanes is sometimes difficult because the domains almost lie under the surfaces, especially poly(ether urethane)s. A very sharp tip is needed to get good results. In this study, the tip radius of 10 nm was used. Under this measurement condition, rough sample has a certain extent influence on the results, but the influence mainly exists the edge of the domains. It has been shown

Table 4
Atomic percentage of carbon, fluorine, oxygen and nitrogen at the depth of about 5 nm on the fluoropolyurethanes film surface

	PEU	FPEU20	FPEU50	FPEU100	PHPCPU	FPHPCPU20	FPHPCPU50	FPHPCPU100
C%[a]	94.0	32.2	41.7	44.3	77.7	46.8	37.7	43.4
O%	6.0	9. 5	11. 3	9.8	20.2	14.0	9. 9	10.4
F%	0	39.4	32.3	32.6	0	26.4	36.4	29.0
N%	0	1.8	2.3	2.6	2.1	2.7	2.9	3.3
C/O	15.7	3.4	3.7	4.5	3.8	3.3	3.8	4.2
F/O	0	4.1	2.9	3.3	0	1.9	3.7	2.8
F/C	0	1.2	0.8	0.7	0	0.6	1.0	0.7
StioichF[b]/C	0	0.034	0.087	0.17	0	0.036	0.091	0.2
K[c]	–	35.3	9.2	4.0	–	16.7	11.0	3.5

[a] The atomic percentage of carbon doesn't contain the percentage of the carbon (CF_2 and CF_3).
[b] F% is shown in Table 1.
[c] K is fluorine enrichment factor ([measured atomic F/C ratio]/[stoichiometric F/C ratio]).

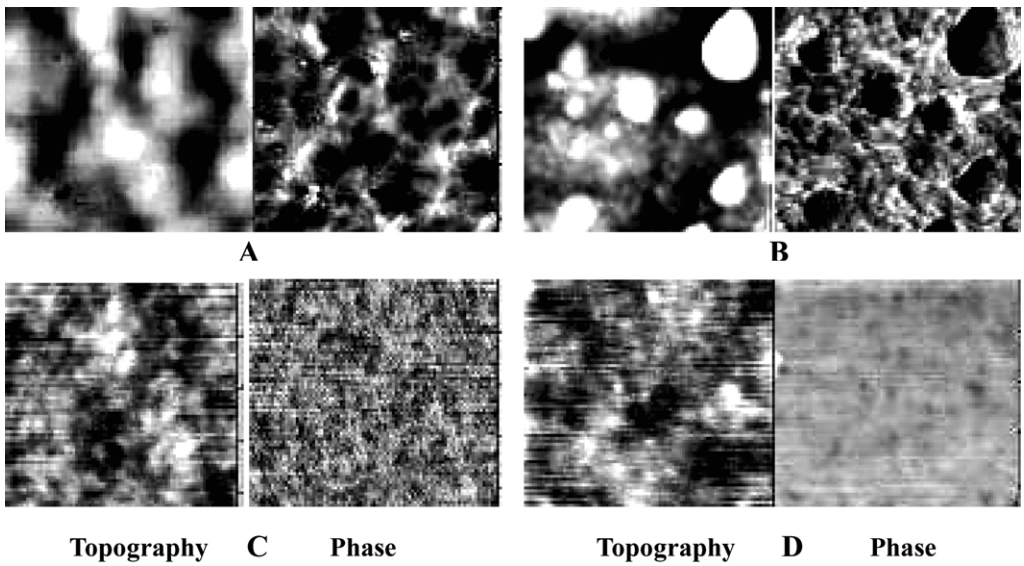

Fig. 7. Topography and phase images of PEU (A), FPEU20 (B), FPEU50 (C), FPEU100 (D) at 1 μm scan sizes. Data obtained using light tapping mode in air. *Z* ranges are 20, 76, 5, 6 nm in A–D, respectively. Phase *Z* ranges are 14.3, 4.7, 0.7, 3.0° in A–D, respectively.

that fluorinated side chains can easily migrate to the surface of polyurethane and are mainly enriched about 0–5 nm below the surface. In order to further understand the effect of fluorinated side chain attached on hard segment on the surface topography of polyurethanes, the light tapping mode AFM was used to study the surface of these fluorinated polyurethanes. Fig. 7 shows the topographic and phase images of PEU, FPEU20, FPEU50 and FPEU100 samples at 1000 nm scan region. For these fluorinated poly(ether urethane)s, FPEU20 gives apparent topographical data on the surface where the hydrophobic patches (rich fluorine patches) appear as low spots, and the hydrophilic areas appear as high spots (Fig. 7B). The phase data for the hydrophobic patches are bright and the hydrophilic areas are dark [37,38]. But hydrophobic and hydrophilic areas of FPEU50 and FPEU100 are not obviously observed in the topography and phase images (Fig. 7C and D). The PEU surface exhibits apparent hydrophobic areas based on the topography and phase images because of the high C/O atomic ratio (Table 4, Fig. 7A). These results suggest that phase separation exists on the surfaces of fluorinated poly(ether urethane)s (FPEU20), and the degree of the phase separation decreases with increasing content of fluorine attached on hard block.

For the fluorinated poly(carbonate urethane)s, FPHPCPU50 and FPHPC100 samples give apparent topography and phase images (worm-like 20 nm width) of hydrophobic rich fluorine patches on their surfaces (Fig. 8C and D). The FPHPCPU20 sample also gives the hydrophobic areas, but there is no distinct phase separation on the surface (Fig. 8B). The surface of PHPCPU sample shows hydrophilic areas from topography and phase images due to the low C/O atomic ratio (Table 4, Fig. 8A). These results suggest that the phase separation on the surface increases with increasing content of fluorine attached on hard block.

3.3. The role of hydrogen bonding in fluorinated polyurethanes

3.3.1. FTIR analysis

Now it is logical to ask way one observes the opposite effect of fluorinated side chain attached on hard segment on the phase separation and surface topography for fluorinated poly(carbonate urethane)s and fluorinated poly(ether urethane)s. That is: the phase separation between hard segments and soft segments increases in fluorinated poly(carbonate urethane)s and decreases in fluorinated poly(ether urethane)s as increasing of fluorine content. One effect could be the change of hydrogen bonding after introduction of fluorine in these two systems. For this reason, FTIR experiments were carried out. Hydrogen bonding exists in polyurethanes, and involves the amide group as the donor, and the urethane carbonyl, the ether oxygen (in polyetherurethanes), or the carbonate carbonyl (in polycarbonateurethanes) as the acceptor. The FTIR spectra of sets of fluoropoly(ether urethane)s samples cast on KBr disc from THF are shown in Fig. 9. A single stretching band is observed near $\sim$3324 cm^{-1} corresponding to the hydrogen-bonded N–H stretching vibration [42]. A free (not hydrogen-bonded) N–H stretching band absorbing 3400–3500 is weakly observed in all samples. This indicates that most of the amide groups in fluoropoly(ether urethane)s are involved in hydrogen bonds [42,43]. The stretching band at $\sim$1730 cm^{-1} is due to the absorption of the free carbonyl of hard segments, and $\sim$1703 cm^{-1} is mainly caused by hydrogen-bonded carbonyl absorption between hard segments [42,44]. Table 5 lists the fraction of hydrogen-bonded carbonyl of urethane according to the relative area of the free carbonyl adsorption and the hydrogen-bonded carbonyl in urethane to calculation [10]. One observes an increasing of carbonyl group absorption at

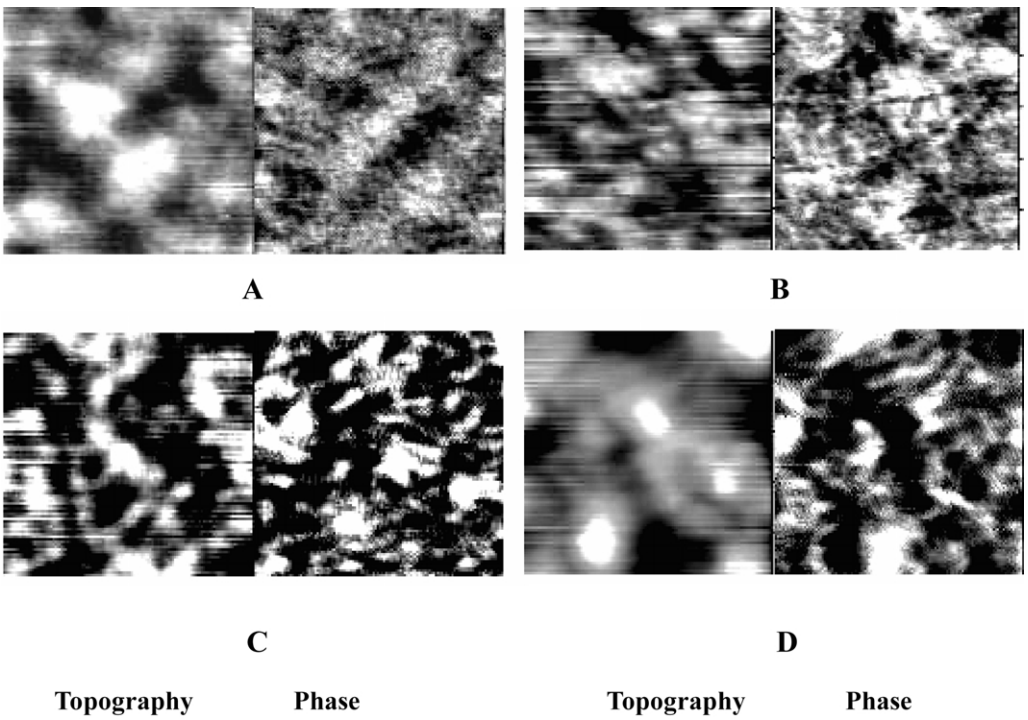

Fig. 8. Topography and phase images of PHPCPU (A), FPHPCPU20 (B), FPHPCPU50(C), FPHPCPU100 (D) at 500 nm scan sizes. Data obtained using light tapping mode in air. *Z* ranges are 5, 9, 6, 18 nm in A–D, respectively. Phase *Z* ranges are 1.4, 2.3, 2.0, 1.6° in A–D, respectively.

$\sim$1730 cm^{-1}, companied with a decreasing of hydrogen-bonded carbonyl group absorption at $\sim$1703 cm^{-1}, with increasing fluorine content (Table 5, Fig. 10). This result suggests that the degree of hydrogen bonding between hard block and soft block is increased as the content of fluorine attached on hard block increases. This will result in an enhanced mixing between soft and hard segments.

A different result is seen for fluropoly(carbonate urethane)s, which is shown in Fig. 11. Here again, almost all the amide groups in fluoropoly(carbonate urethane)s are involved in hydrogen bonding the same as in fluoropoly(ether urethane)s. Fig. 12. shows the 1800–1650 cm^{-1} region assigned to the urethane and carbonate C=O of the fluoropoly(carbonate urethane)s, the stretching band at the 1800–1650 cm^{-1} region is overlapped by the stretching band at $\sim$1743, $\sim$1730, $\sim$1720 and $\sim$1700 cm^{-1} due to

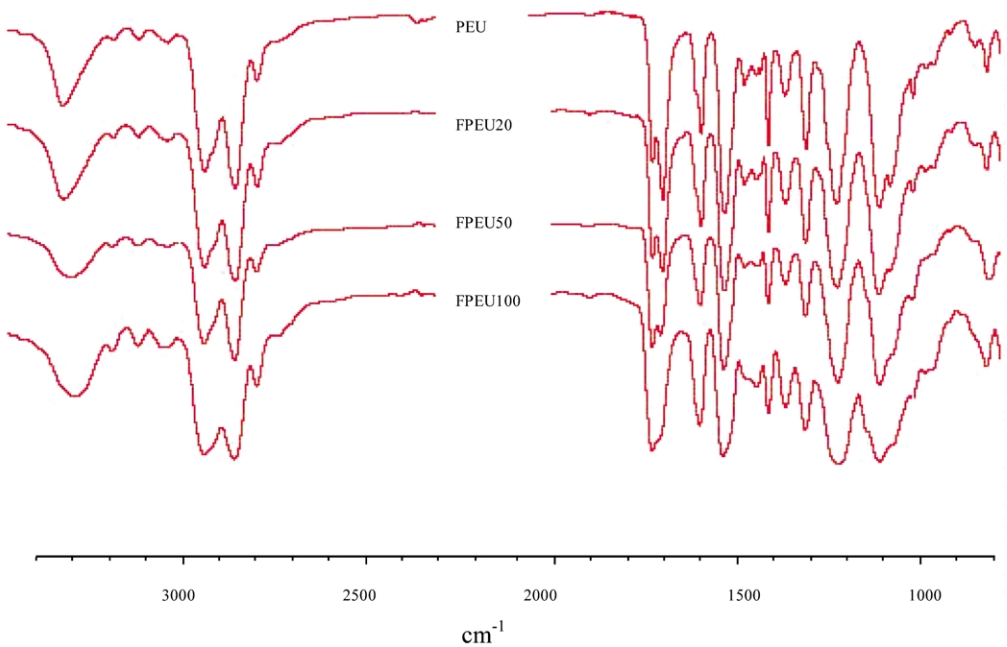

Fig. 9. IR spectra of fluoropoly(ether urethane)s and poly(ether urethane)s.

Table 5
Fraction of hydrogen-bonded carbonyl of urethane and hydrogen-bonded carbonyl of carbonate in FTIR analysis of fluorinated polyurethanes and polyurethanes

	N–H stretching band		Urethane bonded C=O			Carbonate bonded C=O	
	ν (cm^{-1})	$\Delta\nu$[a]	Stretching band ν (cm^{-1})	$\Delta\nu$[a]	(%)	Stretching band (cm^{-1})	(%)
PEU	3328	–	1703	–	78.7	–	–
FPEU20	3325	−3	1704	1	77.0	–	–
FPEU50	3305	−23	1708	5	67.1	–	–
FPEU100	3295	−33	1710	7	73.8	–	–
PHPCPU	3337	–	1693[b]	–	34.6	1723[b]	50.9
FPHPCPU20	3339	2	1700[b]	7	8.1	1720[b]	86.5
FPHPCPU50	3337	0	1700[b]	7	49.5	1720[b]	22.8
FPHPCPU100	3324	−13	1718[b]	25	32.3	1720[b]	55.4

[a] $\Delta\nu = \nu_{FPU} - \nu_{PU}$.
[b] The peak position was obtained by curve fit.

the absorption of the free carbonyl of PHPCD soft segments, free carbonyl of urethane, hydrogen-bonded carbonyl in carbonate and hydrogen-bonded carbonyl absorption of urethane, respectively [3,42–44]. With increasing of fluorine content, the hydrogen-bonded carbonyl adsorption of urethane increases and adsorption of free carbonyl in carbonate at ~1720 cm^{-1} decreases, and the peak (1800–1650 cm^{-1}) becomes sharper (Table 5, Fig. 12) [3,10]. These results suggests that the phase separation is enhanced with increasing of fluorine content because of the fraction of hydrogen-bonded carbonyl increasing and the fraction of free carbonyl in carbonate decreasing in this system.

In addition, the hydrogen-bonded amide group peak position is shifted to lower frequencies, and the hydrogen-bonded carbonyl of urethane peak position is reversely changed with increasing fluorine content in poly(ether urethane) system (Fig. 10, Table 5). However, in poly (carbonate urethane) system, only the hydrogen-bonded amide group peak position of FPHPCPU100 is shifted to low frequencies, all of the hydrogen-bonded carbonate carbonyl peak position are almost same, and that of hydrogen-bonded carbonyl of urethane increases with

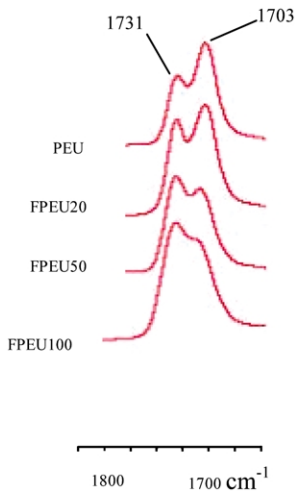

Fig. 10. Urethane C=O stretching region [A] of fluoropoly(ether urethane)s and poly(ether urethane)s.

increasing fluorine content, especially, the frequency shift $\Delta\nu$ of FPHPCPU100's is 22 cm^{-1} compared to PHPCPU's (Table 5). According to Schrems' result [45], the frequency shift might be ascribed to the matrix effect derived from the polarity difference between soft segment rich and hard segment rich domains, and the magnitude of the frequency shift $\Delta\nu$ is a measure of hydrogen bonding strength. Therefore, it can be known through investigating hydrogen bonding strength of urethane that fluorinated side chain attached on hard segment influences the bulk phase separation and surface topography in different way for these two sets of fluorinated polyurethane systems. We take FPEU100 and FPHPCPU100, for instance, to discuss these effects because they only contain PFOPDOL chain extender. It is interesting to note that the shift $\Delta\nu$ (25 cm^{-1}) of hydrogen bonded carbonyl in FPHPCPU100 is higher than that ($\Delta\nu = 7$ cm^{-1}) in FPEU100, and that the frequency shift ($\Delta\nu = -13$ cm^{-1}) of amide group in FPHPCPU100 is far lower that ($\Delta\nu = -33$ cm^{-1}) in FPEU100 (Table 5). However, there is almost constant peak position of the ether bond (~1105 cm^{-1}) in poly(ether urethane)s (Fig. 9) and the carbonyl in carbonate (Table 5, Fig. 12). These results indicate that the acceptor strength of carbonyl in urethane is increased in polycarbonate matrix and the donor strength of the amide group is increased in polyether matrix. The increasing acceptor strength of carbonyl in urethane promotes the phase separation. On the contrary, the increasing donor strength of amide group is helpful to enhance phase mixing.

4. Conclusion

In summary, DSC, DMA measurements on fluorinated poly(ether urethane)s and fluorinated poly(carbonate urethane)s containing various amounts of chain extender of fluorinated side chains clearly show that the bulk phase separation increases in fluorinated poly(carbonate urethane)s and the phase mixing increases in fluorinated poly(ether urethane)s with increasing amounts of fluorinated

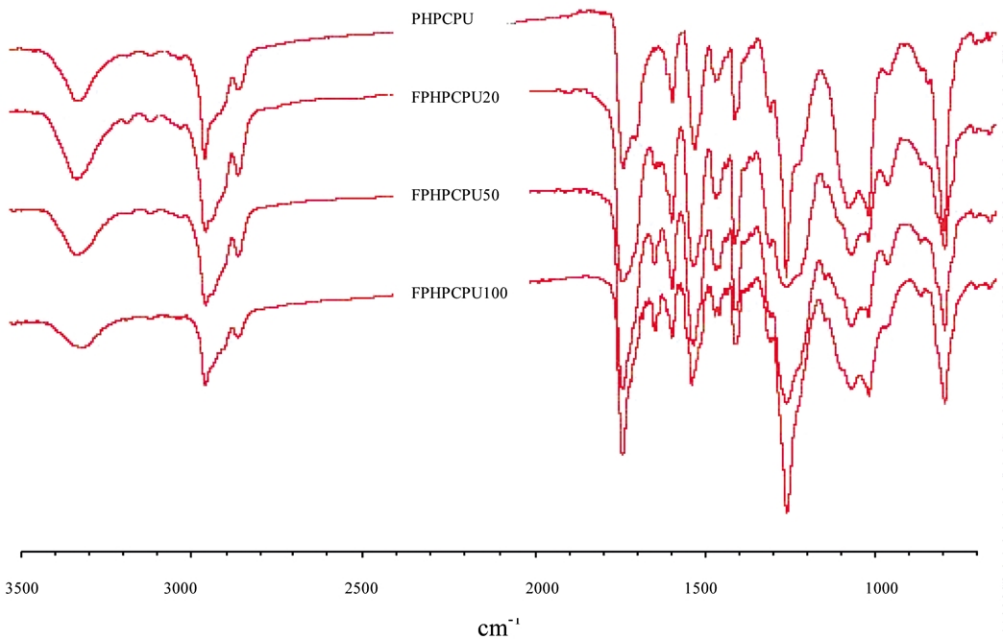

Fig. 11. IR spectra of fluoropoly(carbonate urethane)s and poly(carbonate urethane)s.

side chain on hard segment. It is evidenced by AFM and XPS that the change of surface phase separation is same as that of the bulk phase separation in fluorinated poly(ether urethane)s and fluorinated poly(carbonate urethane)s. The increased degree of hydrogen bonding between hard segments and soft segments is evident by FTIR for fluorinated poly(ether urethane), and the enhanced association of domains with long-range order (hydrogen bonding) between hard segments for fluorinated poly(carbonate urethane)s. The result is new and provides direct evidence that the surface topography of these fluorinated polyurethanes depends strongly on the extent of the phase separation in bulk. The fluorinated side chain influences the phase separation and surface topography of polyurethanes due to its ability of forming hydrogen bonding depending on soft segments. These studies will be advantageous to designing fluorinated polyurethanes with special surface structure and function, and provides a fine model for investigating the importance of polyurethane microdomain structure on protein adsorption and blood platelet interaction [46].

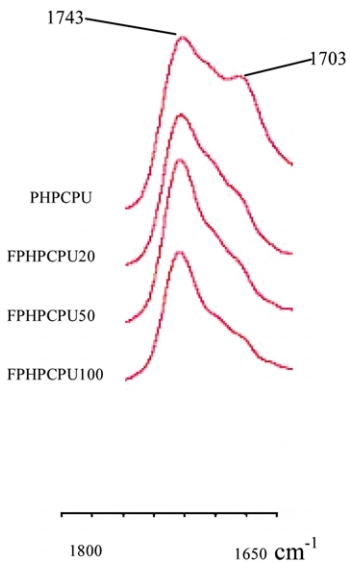

Fig. 12. Urethane C=O stretching region [A] of fluoropoly(carbonate urethane)s and poly(carbonate urethane)s.

Acknowledgements

We would like to express our great thanks to the China National Distinguished Young Investigator Fund (29925413) and National Natural Science Foundation of China (50303014 and 59973013) for Financial Support. We would also like to thank Mr Yunfei Tian, Center of Analysis, Sichuan University, for AFM measurement.

References

[1] Boretos JW, Pierce WS. Science 1967;158:1481.
[2] Adhikari R, Gunatillake PA, McCarthy SJ, Meijs GF. J Appl Polym Sci 2000;78:1071.
[3] Tang YW, Labow RS, Santerre JP. J Biomed Mater Res 2001;56:516.
[4] Sung CSP, Smith TW, Sung NH. Macromolecules 1980;13:117.
[5] Martin DJ, Meijs GF, Gunatillake PA, McCarthy SJ, Renwick GM. J Appl Polym Sci 1997;64:803.
[6] Wang CB, Cooper SL. Macromolecules 1983;16:775.
[7] Aitken RR, Jeffs GMF. Polymer 1977;18:197.
[8] Seymour RW, Cooper SL. Macromolecules 1973;6:48.
[9] Leung LM, Koberstein JT. Macromolecules 1986;19:706.
[10] Miller JA, Lin SB, Kirk KS, Hwang KKS, Wu KS, Gibson PE, Cooper SL. Macromolecules 1985;18:32.

[11] Chapman TM, Benrashid R, Marra KG, Keener JP. Macromolecules 1995;28:331.
[12] Chapman TM, Marra KG. Macromolecules 1995;28:2081.
[13] Akemi H, Aoyagi T, Shinohara I, Okano T, Kataoka K, Sakurai Y. Makromol Chem 1986;187:1627.
[14] Kaku M, Grimminger LC, Sogah DY, Haynie SL. J Polym Sci Part A: Polym Chem Ed 1994;32:2187.
[15] Zhemovay LN, Galatenko NA, Hkranovskiy VA. Kompoz Polim Mater 2000;22:26.
[16] Chen KY, Kuo JF. Macromol Chem Phys 2000;201:2676.
[17] Schmidt DL, Coburn CE, Dekoven BM, Potter GE, Mayers GF, Fischer DA. Nature 1994;368:39.
[18] Zhuang H-Z, Marra KG, Ho T, Chapman TM, Gardella Jr JA. Macromolecules 1996;29:1660.
[19] Akhremitchev BB, Monney BK, Marra KG, Chapman TM, Walker GC. Langmuir 1998;14:3976.
[20] Game P, Sage D, Chapel JP. Macromolecules 2002;35:917.
[21] Kim YS, Lee JS, Ji Q, McGrath JE. Polymer 2002;43:7161.
[22] Yoon SC, Ratner BD. Macromolecules 1986;19:1068.
[23] Yoon SC, Ratner BD. Macromolecules 1988;21:2392.
[24] Yoon SC, Ratner BD. Macromolecules 1988;21:2401.
[25] Yoon SC, Ratner BD, Ivan B, Kennedy JP. Macromolecules 1994;27: 1548.
[26] Yoon SC, Sung KS, Ratner BD. Macromolecules 1990;23:4351.
[27] Honeychuck RV, Ho T, Wynne KJ, Nissan RA. Chem Mater 1993;5: 1299.
[28] Revenko I, Tang Y, Santerre JP. Surf Sci 2001;491:346.
[29] Mclean RS, Sauer BB. Macromolecules 1997;30:8314.
[30] Tonelli C, Trombetta T, Scicchitano M, Simeone G, Ajroldi G. J Appl Polym Sci 1996;59:311.
[31] Tonelli C, Ajroldi G, Turturro A, Marigo A. Polymer 2001;42:5589.
[32] Tonelli C, Ajroldi G, Marigo A, Marego C, Turturro A. Polymer 2001; 42:9705.
[33] Thomas HR, O'Malley JJ. Macromolecules 1979;12:323.
[34] O'Malley JJ, Thomas HR, Lee GM. Macromolecules 1979;12:996.
[35] Tan H, Xie XY, Li JH, Zhong YP, Fu Q. Polymer. Accepted for publication.
[36] Magonov SN, Elings V, Whangbo MH. Surf Sci 1997;375:385.
[37] Brandsch R, Bar G, Whangbo MH. Langmuir 1997;13:6349.
[38] Sauer BB, Mclean RS, Thomas RR. Langmuir 1998;14:3045.
[39] Briggs D. Surface analysis of polymers by XPS and static SIMS. Cambridge: Cambridge University Press; 1998. Chapter 2.
[40] Kissa E. Fluorinated surfactants: synthesis, properties, applications. New York: Marcel Dekker; 1993. p. 386.
[41] Ming W, Laven J, Linde R. Macromolecules 2000;33:6886.
[42] Srichatrapiumuk VW, Cooper SL. J Macromol Sci Phys 1978;B15: 267.
[43] Coleman MM, Skrovanek DJ, Hu J, Painter PC. Macromolecules 1988;21:59.
[44] Coleman MM, Skrovanek DJ, Hu J, Painter PC. Macromolecules 1985;18:32.
[45] Schrems O, Oberhoffer HM, Luck WAP. J Phys Chem 1984;88:4335.
[46] Tingey KG, Andrade JD. Langmuir 1991;7:2471.